Quantitative interpretation using inverse rock-physics modeling on AVO data

Erling Hugo Jensen[1], Tor Arne Johansen[2, 3, 4], Per Avseth[5, 6], and Kenneth Bredesen[2, 7]

Abstract

Quantitative seismic interpretation has become an important and critical technology for improved hydrocarbon exploration and production. However, this is typically a resource-demanding process that requires information from several well logs, building a representative velocity model, and, of course, high-quality seismic data. Therefore, it is very challenging to perform in an exploration or appraisal phase with limited well control. Conventional seismic interpretation and qualitative analysis of amplitude variations with offset (AVO) are more common tools in these phases. Here, we demonstrate a method for predicting quantitative reservoir properties and facies using AVO data and a rock-physics model calibrated with well-log data. This is achieved using a probabilistic inversion method that combines stochastic inversion with Bayes' theorem. The method honors the nonuniqueness of the problem and calculates probabilities for the various solutions. To evaluate the performance of the method and the quality of the results, we compare them with similar reservoir property predictions obtained using the same method on seismic-inversion data. Even though both approaches use the same method, the input data have some fundamental differences, and some of the modeling assumptions are not the same. Considering these differences, the two approaches produce comparable predictions. This opens up the possibility to perform quantitative interpretation in earlier phases than what is common today, and it might provide the analyst with better control of the various assumptions that are introduced in the work process.

Introduction

Seismic amplitude variations with offset (AVO) for reflections between two layers depend on the elastic properties and densities of both layers, which in turn are affected by hydrocarbon saturation and lithology. These amplitude variations can be modeled using the Zoeppritz equations (Mavko et al., 2009). AVO can be used as a direct hydrocarbon indicator by studying the intercept R_p crossplotted versus the gradient G. Typically, the data will exhibit a background trend of decreasing G with increasing R_p, and a fluid factor can be defined as the perpendicular distance from this projection line to the data (Smith and Gidlow, 1987).

Figure 1 shows the fluid factor for a vertical seismic section from the Norwegian Sea, slicing through and extending beyond a gas-sandstone discovery well (black dashed line). The fluid factor has been used to identify possible hydrocarbon prospects on the section. For example, we identify the hydrocarbon reservoir formations as well as some brightening right below the base Cretaceous unconformity (BCU) when moving off the structural high. Farther north, however, the graben anomalies have proven to be false (Avseth et al., 2016). Similarly, more detailed interpretation maps can be produced by highlighting various facies using the intercept versus gradient crossplot. Nevertheless, it is still a coarse interpretation method not suitable for quantitative interpretation.

Quantitative predictions of physical parameters from prestack seismic data can be done through AVO inversion. For this,
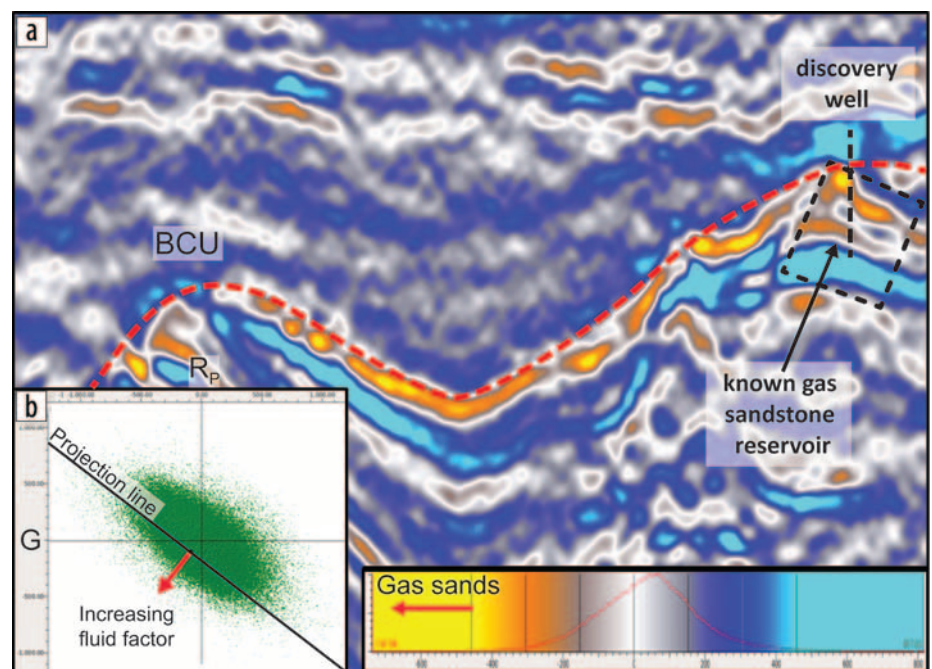

Figure 1. Vertical section covering and extending beyond a known gas-sandstone reservoir in the Norwegian Sea, showing (a) negative fluid factor for top response plotted in yellow (while bottom response of reservoir is positive and plotted in blue) and (b) crossplot of R_p versus G used in deriving the fluid factor.

[1]Rock Physics Technology.

[2]Department of Earth Science, University of Bergen, Norway.

[3]The University Centre in Svalbard, Norway.

[4]ARCEx Research Centre for Arctic Petroleum Exploration, The Arctic University of Norway.

[5]Tullow Oil.

[6]Norwegian University of Science and Technology.

[7]Spike Exploration.

various approximations of the Zoepptriz equations are used, each with specific assumptions and limitations. Typical predicted parameters are acoustic impedance and V_P/V_S ratio, acoustic and elastic impedance, or the product of Lamé's parameter, lambda times density and shear modulus times density (Avseth et al., 2005). Many different methods can be applied in AVO inversion, including stochastic and probabilistic types of inversions, which use Bayes' theorem (Tarantola, 2005). Geostatistical methods can then be applied when combining the predicted properties with measurements from well logs for quantitative interpretation of the reservoir quality.

The inverse rock-physics modeling (IRPM) approach of Johansen et al. (2013) is a generic method for predicting reservoir parameters, such as porosity, lithology, and fluid saturation, from various types of inputs and rock-physics models. It has been demonstrated previously on well-log and seismic-inversion data. In this paper, we extend IRPM to use AVO data as input for direct quantitative prediction of reservoir parameters. Here, we have assumed an interface between a cap rock with known elastic properties and a layer for which properties are modeled using the chosen rock-physics model; the predicted reservoir parameters are for this second layer. Hence, IRPM on AVO data makes predictions located at the interface *between the layers*, while IRPM on seismic data makes predictions at each *specific subsurface location*. To evaluate the performance of this new type of AVO IRPM, we compare the results with results that use IRPM on seismic-inversion data.

Inverse rock-physics modeling on AVO data

Johansen et al. (2013) showed how inverse rock-physics modeling (IRPM) can give physically consistent predictions of porosity, lithology, and fluid saturation (PLF) from, e.g., acoustic impedance and V_P/V_S ratio. This is a nonlinear and underdetermined problem with nonunique solutions. In IRPM, the predictions are obtained making an exhaustive search in so-called forward-modeled constraint cubes for PLF properties matching the input data. Bredesen et al. (2015) demonstrated the use of IRPM on seismic-inversion data, where uncertainties in input and model data were handled using probability density functions and a Monte Carlo simulation in the forward-modeling step of the constraint cubes. Probabilities

of how well the data fit the model for the joint predictions of the PLF parameters can then be calculated. Using the definitions by Cooke and Cant (2010), this variation of IRPM can be described as a stochastic and probabilistic type of inversion.

In this study, we extend IRPM to use AVO data as input. While IRPM on seismic-inversion data reflects properties at subsurface locations, IRPM on AVO data makes predictions at the interfaces between two layers. The predictions depend on the properties of the layer above and below the interface, referred to as top and bottom layers, respectively. Therefore, we extend the forward modeling of the constraint cubes to use fixed properties for one of the layers, while the properties of the other layer are modeled using a rock-physics model with a range of possible PLF. For example, when considering the interface between the cap rock and the reservoir, we assign fixed cap-rock properties to the top layer and the reservoir rock-physics model to the bottom layer. Forward-modeled intercept R_P and gradient G constraint cubes shown in Figure 2 are then calculated according to

$$R = \frac{Z_2 - Z_1}{Z_2 + Z_1} \text{ and } G = R_p - 2R_s ,\qquad(1)$$

where R, Z_1, and Z_2 are normal reflection coefficient and acoustic impedances for the top and bottom layers, respectively. The P-wave and S-wave normal reflection coefficients (R_p and R_s) are calculated using P- and S-wave impedances, respectively.

Figure 3 shows an example in which we have applied IRPM to AVO data for a synthetic wedge model with a 25 Hz Ricker wavelet. The layer properties are equivalent to those for the known reservoir in the Norwegian Sea data set, which is used for demonstration of the method later in this paper. Specifically, the reservoir rock properties have been estimated using the representative rock-physics model given a porosity, lithology, and gas saturation of 0.24, 0, and 1, respectively. We will use the synthetic example to explain the various steps in the modeling.

First, we have extracted the AVO data from angle gathers, simply using far- versus near-stack attributes (Avseth et al., 2008), where uncalibrated R_p is set equal to the near-stack data and
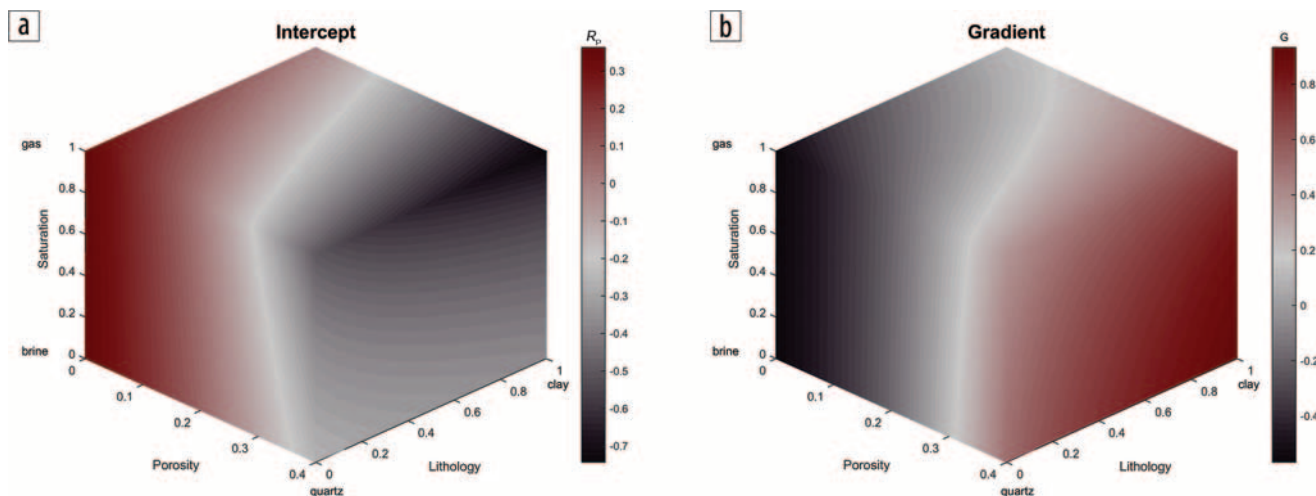

Figure 2. Forward-modeled rock-physics constraint cubes for (a) intercept R_p and (b) gradient G. The varying porosity, lithology, and saturation are the reservoir properties of the layer below the interface, i.e., bottom layer.

uncalibrated G is estimated from far-stack minus near-stack data, where the far stack has been properly balanced relative to the near stack (see Figure 3a). However, this results in relative AVO data, i.e., $R_{p,relative}$ and $G_{relative}$. For IRPM we need absolute (or scaled) values. A typical approach is to use modeled synthetic seismograms in a well position. An alternative method is to perform variance or covariance matching of modeled and observed background trends (Avseth et al., 2003). In this study, we use a simple scalar correction to estimate the absolute or scaled AVO attributes:

$$R_{p, scaled} = f_R \cdot R_{p, relative} \text{ and } G_{scaled} = f_G \cdot G_{relative}, \quad (2)$$

where f_R, f_G, $R_{p,scaled}$, and G_{scaled} are scaling factors and scaled R_p and G, respectively. More generally, when R_p and G are derived from least-squares regressions and therefore are interdependent, the correction may involve a mixing of the two reflectivities: $G_{scaled} = f_{G1} \cdot G_{relative} + f_{G2} \cdot R_{p, relative}$. However, such mixing corrections are outside the scope of this paper, and we will only use single scaling factor as a first-order correction, which is less data demanding and appropriate in an exploration setting. Still, the calibration of the scaling factors is critical, as it governs the possibility of using rock-physics models to correlate reservoir properties to the AVO attributes. For this, we utilize rock-physics templates (Avseth et al., 2005) and "extend" these to the R_p - G domain (see Figure 3b). In the synthetic case, the calibration process is trivial as we have full control over all the parameters; we adjust the scaling factors to achieve a good fit between the green data point (representative of the response at the interface) and a modeled R_p and
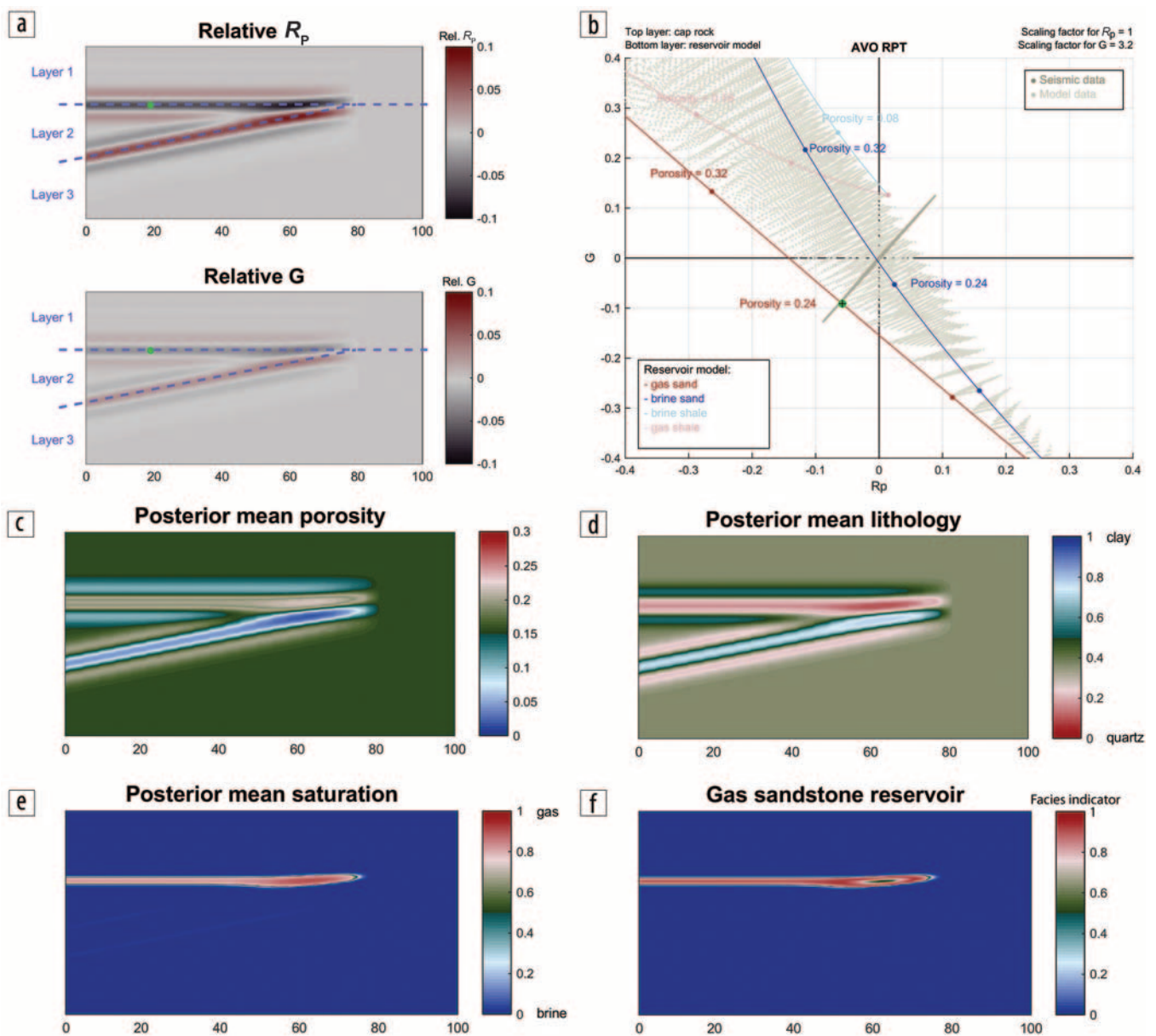

Figure 3. Example of AVO IRPM on synthetic wedge model, showing (a) relative R_p and G for wedge model with density = 2.5 g/cm³, V_P = 2.9 km/s and V_S = 1.6 km/s for layer 1 and 3 (cap rock), and density = 2.1 g/cm³, V_P = 3.1 km/s and V_S = 2.0 km/s for layer 2 (reservoir rock); (b) rock-physics template in the AVO domain, posterior mean; (c) porosity; (d) lithology; and (e) gas saturation; and (f) is the facies indicator of gas-saturated sandstone when combining the results from interchanging the top- and bottom-layer properties in the AVO IRPM model.

G (black cross) with the same porosity, lithology, and fluid saturation.

When working with actual seismic data, this calibration step is more challenging. But if one extracts a subset of data close to the well location, a similar approach can be applied. The template lines, e.g., the red line, which shows modeled gas-saturated sandstones for the bottom layer with varying porosity, can be used as a guideline in the calibration process. If possible, it is recommended to use groups of data points that are representative for transitions between different sets of facies combined with matching templates, as this will help to constrain the scaling factors. Calibrating the scaling factors can be an iterative process, readjusting the scaling factors after running IRPM on the scaled AVO data in a region with good understanding of the geology. As the synthetic case shows, we can have data that extend beyond the saturated sandstone model line. This might be due to interference, e.g., because of tuning effects, as is the case here. But it also might be related to differences in the top- and bottom-layer properties compared to the specifications in our model. Once the calibration process is performed on the data subset, the scaling factors are applied to the whole data set, assuming all the data have the same survey and processing specifications.

Except for this scaling procedure and the extension to the constraint cubes, the IRPM process is generic and independent of having AVO or seismic-inversion data as input. In both cases, we define a prior probability for brine saturation to be 99.5%; the remaining probability density is given by a mean, standard deviation, minimum, and maximum value of 0.7, 0.19, 0, and 1, respectively. Our reasoning behind this prior is, in general, that the probability for brine is much higher than hydrocarbon saturation. In addition, the variance in fluid saturation is typically larger when making predictions of brine-saturated compared to hydrocarbon-saturated rocks. Hence, with a relatively good match between the data and the model for a brine-saturated rock, this prior will favor a prediction of brine saturation. We use the principle of indifference when specifying the prior for porosity and lithology to be equal in the range from 0 to 0.4 and 0 to 1.0, respectively. But because IRPM is a coupled type of inversion, the brine saturation prior will also have implications for predicted lithology and porosity; e.g. for a brine-saturated rock, they will be less influenced by results correlating with higher hydrocarbon saturations and therefore will yield a more physically consistent result.

The Bayesian probability $P(\phi,c,s|M_0,d)$ for a solution with a combination of porosity, ϕ, lithology, c, and fluid saturation, s, given a particular model, M_0, and data, d, is calculated using Bayes formula:

$$P(\phi,c,s|M_0,d) \propto P(d|M_0,\phi,c,s)P(\phi,c,s). \qquad (3)$$

To evaluate the solutions, we calculate the posterior mean porosity, lithology, and saturation. For the wedge model, they are shown in Figure 3c, d, and e. We see a clear response at the interface between the cap rock and the reservoir. The effect of the side lobes is quite visible, but the predictions (in the center) at the actual interface match quite well with the reservoir model. We also notice an increase in predicted porosity, volume fraction of sand, and gas saturation where we have the tuning effect.

Finally, we define a facies indicator, which is the product of the posterior distribution and the largest posterior probability to a solution within the facies specifications. In our modeling, we have used facies specifications for a gas-sandstone facies (GSF) to have porosities between 0.1 and 0.35, clay volume fractions between 0 and 0.4, and gas saturations between 0.60 and 1.0. Hence, high probabilities for gas sandstones need to satisfy two main criteria: (1) within the model space, it is more likely to be a GSF than not, and (2) there exists at least one solution within GSF which gives a good match between the data and the model. For the wedge model, the AVO IRPM GSF predictions are consistent with the model (see Figure 3f), except where the tuning effect sets in. There the lines become "hollow" creating a characteristic "eye of the needle" shape because the signal interference has resulted in a decrease in the posterior probability. By inverting the layer order in the AVO IRPM modeling, the results along the wedge will also be inverted. This can be used to estimate the extent of the reservoir layer.

Application to a Norwegian Sea data set

To demonstrate the performance of AVO IRPM, an interpreted horizon might be the intuitive choice. But we believe that AVO analysis should be integrated into the seismic interpretation workflow, and AVO IRPM might help toward achieving that. Therefore, we choose to demonstrate IRPM on a vertical section from a Norwegian Sea data set covering and extending beyond a discovered mid-Jurassic gas-sandstone reservoir in the Garn and Ile formations at approximately 2.5 km total depth (Figure 4).

In the well, the thickness of Garn and Ile are approximately 30 m and 60 m, respectively, with a 10 m thick silty-shale, the Not Formation, between them. We will use the modified differential effective medium model (Mavko et al., 2009), which Bredesen et al. (2015) calibrated using the well-log data. In the case of the AVO IRPM, this model is applied to the bottom layer. Data from the discovery well have also been used to calibrate the cap-rock properties. There were some issues with the cap-rock measurements above Garn, but the properties seem fairly similar to those of the Not Formation. Hence, we have mainly used data from the Not Formation to specify the cap-rock properties applied to the top layer, having a mean density, P-, and S-wave velocities of 2.5 g/cm³, 3.0 km/s, and 1.6 km/s, respectively.

We calibrate the AVO scaling factors to be 0.00032, using the AVO rock-physics template on a subset of the vertical section from around the known reservoir (see Figure 5a). The data plotting beyond the gas-sandstone model line are mainly from the interface between the cap rock and Garn. Hence, we have performed our calibration to make this model line fit the data at the interface between Not and Ile. Figure 5b shows the calibrated AVO scaling factor applied to the whole vertical section. Now there are a lot more data that extend beyond the gas-sandstone model line, associated with a higher fluid factor.

Figure 6 shows posterior mean PLF for IRPM on both the AVO and seismic-inversion data. Both approaches predict high porous, gas-saturated sandstones for the known reservoir. They also both predict porous, hydrocarbon-saturated sandstones down into the graben formation, as well as several additional layers beneath it and the known reservoir, some with predicted gas saturation.

In Figure 7, we have plotted the probability for gas-sandstone facies. Both approaches show high probability in the known reservoir formations. But the probability associated with the Garn Formation is lower when using the seismic-inversion data compared to the AVO data as input. We also notice that in both cases the downflank anomalies, which in Figure 6 showed predictions of porous, high gas-saturated sandstones, are now much more fragmented. In case of the AVO IRPM, this is depicted in the shape of "hollow" lines, similar to the results in the synthetic wedge example.

Discussion

AVO IRPM does not use a wavelet or initial velocity model, something other quantitative seismic interpretation methods might require. However, some of the other main assumptions and challenges are addressed below. We have demonstrated IRPM using AVO and seismic-inversion data as input. We cannot directly

compare the results of the two approaches because they will never be identical. For example, the IRPM results will reflect the fact that seismic-inversion data depict properties at a given subsurface location, while AVO data reflect changes in layer properties located at the interface between the layers. Hence, the thickness of each layer is not as easily determined in the case of AVO IRPM compared to the other approach. Furthermore, if the actual top-layer properties deviate from our modeling specifications in the AVO IRPM, the predictions for the two approaches might deviate as well. Keeping in mind these fundamental differences between the two approaches gives a basis for comparing the results between them.

A low-frequency depth trend has been used in the seismic inversion but not in the AVO IRPM. In addition to the lack of interfaces in the overburden, as can be seen from the input data (Figure 4), this might be a reason for differences in IRPM predictions in the overburden. Below BCU, the results of main features
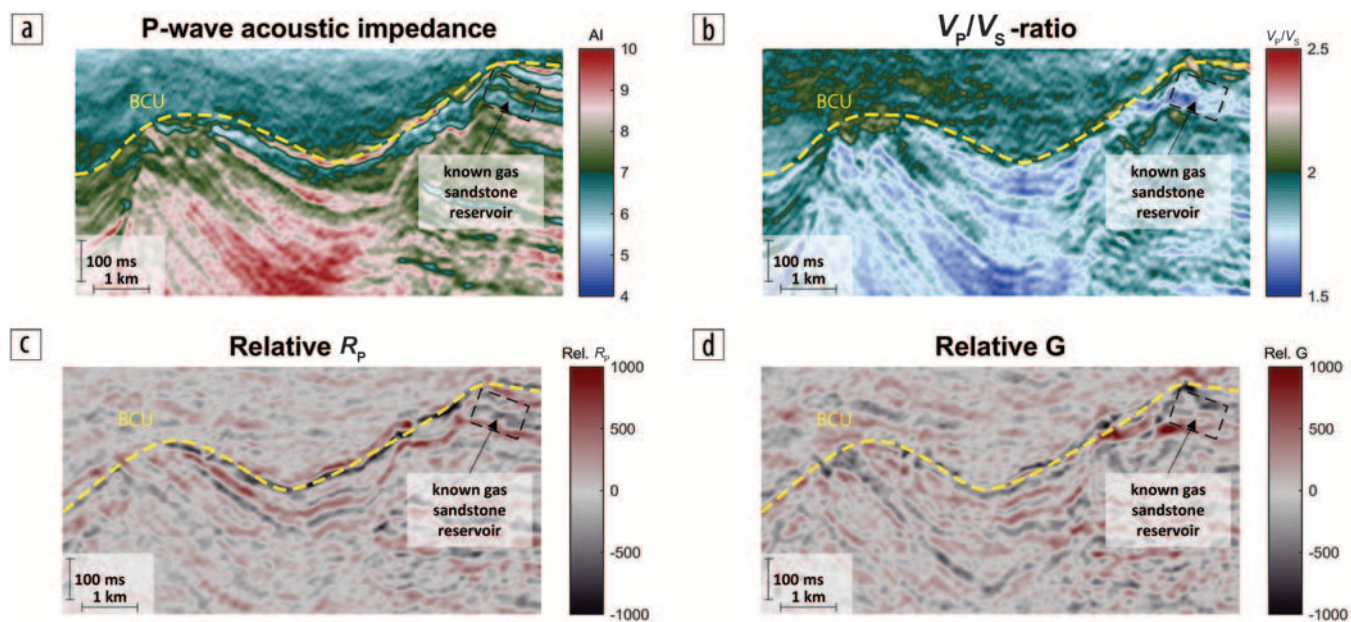

Figure 4. Vertical section covering and extending beyond a known gas-sandstone reservoir in the Norwegian Sea, showing (a) P-wave acoustic impedance, (b) V_P/V_S ratio, (c) relative intercept R_p, and (d) relative gradient G.
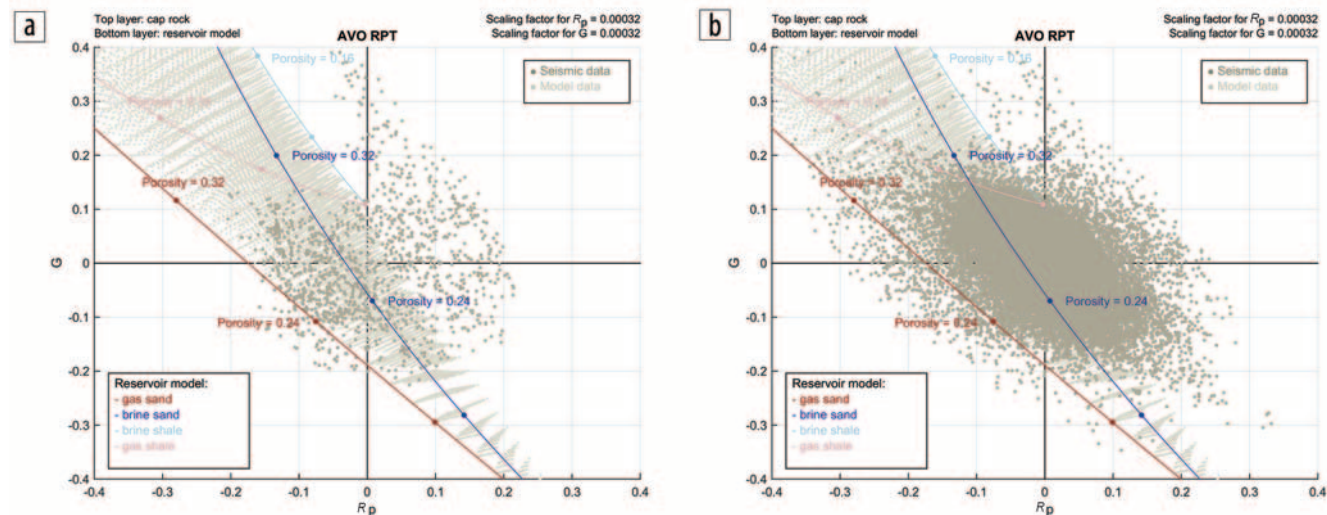

Figure 5. Intercept and gradient data from (a) a subsection of the known reservoir and (b) the whole vertical section, plotted in a rock-physics template.

are in agreement for the most part. For example, the porous sandstone layers beneath dense shale layers and predicted hydrocarbons are comparable; deviation is larger in layers with lower probability of hydrocarbons. Other layer combinations, e.g., gas-water contacts or sandstone above shale, can be tested easily to improve the interpretation even further. Combining such results can be used to estimate layer thicknesses.

The strongest hydrocarbon response beyond the known reservoir was found downflank into the graben formation, but it became fragmented when studying the facies indicator of a gas sandstone. However, testing other properties for the top layer might give a different result. For example, it is believed that the cap rock in the bottom of the graben is either a hard carbonaceous layer or soft organic-rich shale interval. Nevertheless, these anomalies still might be false positives; for example, Avseth et al. (2016) show that the presence of a hard carbonaceous layer in the graben creates refraction energy that interferes with primary reflections on high incidence angles at the target. It is always important to honor local geologic variability during the AVO analysis. Moreover, the data are uncertain and the inversion is also uncertain, nonunique, and will depend on numerous assumptions.

We have used the simple two-term AVO relation in our modeling and approximated R_p and G from near- and far- minus near-angle stacks. More advanced and sophisticated methods, such as AVO regression or reflectivity inversion, might give more accurate

results. However, they typically require higher data quality. For example, the overall attenuation Q-factor compensation in the Norwegian Sea data set is not good enough to do an intercept-gradient inversion. Applying regression on common-depth points (CDPs) can also be more susceptible to noise. Such methods are also more time consuming and resource demanding, and smaller companies might have access only to angle stacks and not the full angle gathers. However, if full angle gathers are available, these should be inspected for quality control of the identified anomalies to verify that they are not due to various artifacts.

Tuning effects and interference due to thin layers is challenging when working with AVO, but the Norwegian Sea data set is broadband data with better resolution and less side lobes compared to conventional seismic data. In the synthetic example, we saw the effect on the AVO response and IRPM predictions where we had a tuning effect at the pinch out of the wedge model, reducing the probability of a gas sandstone. A similar pattern is observed in the graben formation for the Norwegian Sea data set, where interference and other wave propagation effects related to curvature and large velocity contrasts have distorted the far-angle amplitudes (Avseth et al., 2016).

The calibration of the scaling factors for R_p and G is critical. Contrary to the case for the Norwegian Sea data set, in general they will not be the same. But a rescaling of G had been done for this data set prior to our modeling. Without this rescaling, the calibration
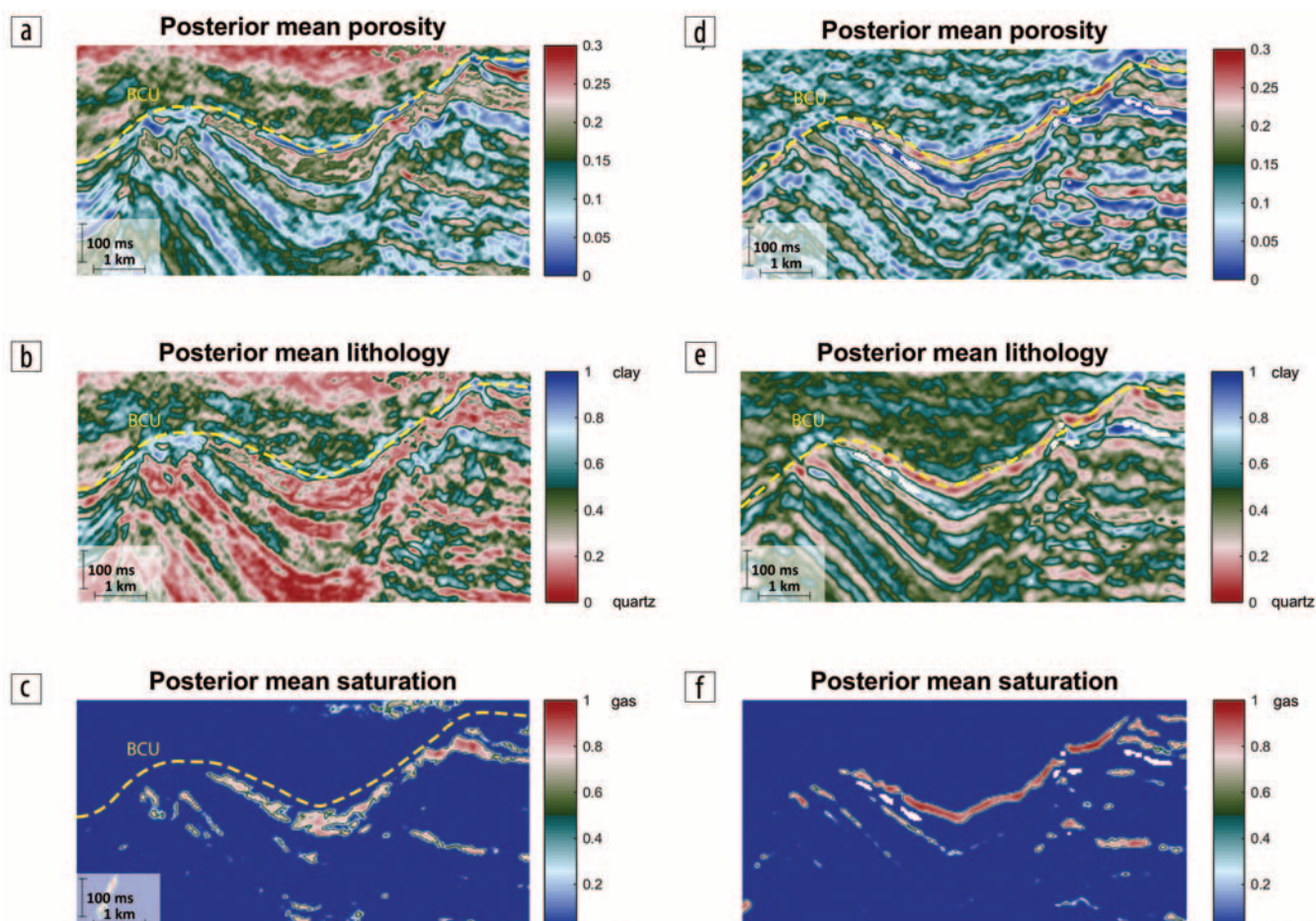

Figure 6. (a) Predicted posterior mean porosity, (b) lithology, and (c) gas saturation when using seismic-inversion data as input and (d), (e), and (f) when using AVO data as input.
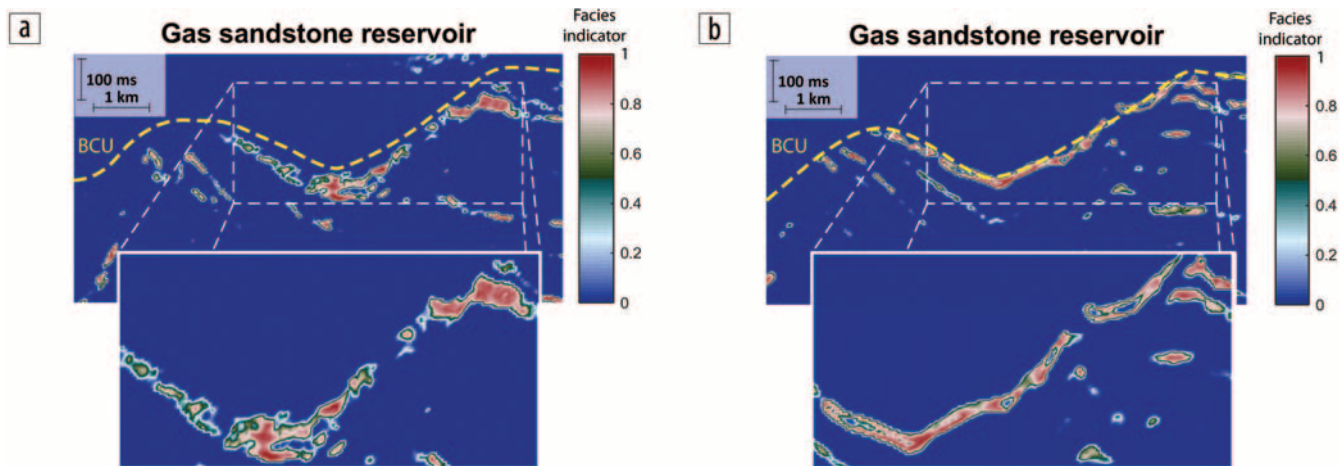
Figure 7. Facies indicator of a gas-sandstone reservoir (a) when using seismic-inversion data as input and (b) when using AVO data as input.

strategy would still be the same: calibrate using rock physics and AVO modeling trend lines on a subset of the data we have good knowledge of, e.g., the interface between the cap rock and the gas-sandstone reservoir at the well location. Finally, we assume the same scaling factors can be applied to the whole section.

The applied rock-physics model has been calibrated against the hydrocarbon reservoir zones based on data from the well log. Hence, the model is best suited for characterizing this type of reservoir sandstone; one needs to be cautious when making predictions away from the known well location. However, because this is a physically and not statistically driven method, we can test various rock types more easily, e.g., accounting for increased cementation and consolidation with increased depth. The physically consistent solutions can then be combined and interpreted to extract more information from existing seismic data in a reservoir prediction process.

Conclusions

We have demonstrated a method using AVO data for reservoir characterizations and compared the results with those we get when using seismic-inversion data. Considering the inherent differences between the two approaches, they yield results in which the main features of facies, porosity, lithology, and fluid saturation predictions are in agreement, despite having used very simple methods for approximating the AVO attributes. In particular, both cases provide good response and quite consistent predictions of the reservoir properties for a gas-sandstone discovery in the Norwegian Sea, which are also in agreement with the well-log measurements. This is a very encouraging result, as AVO data are far more common than seismic-inversion data. Hence, the presented method provides a less resource-demanding alternative for quantitative seismic interpretation. We have shown that this can provide valuable input when doing seismic interpretation, in addition to being useful for reservoir prediction, e.g., to derisk appraisal or exploration wells. **TLE**

Corresponding author: erling.jensen@rptas.no

References

Avseth, P., H. Flesche, and A.-J. van Wijngaarden, 2003, AVO classification of lithology and pore fluids constrained by rock physics depth trends: The Leading Edge, **22**, no. 10, 1004–1011, http://dx.doi.org/10.1190/1.1623641.

Avseth, P., T. Mukerji, and G. Mavko, 2005, Quantitative seismic interpretation: Applying rock physics to reduce interpretation risk: Cambridge University Press, http://dx.doi.org/10.1017/CBO9780511600074.

Avseth, P., A. Dræge, A.-J. van Wijngaarden, T. A. Johansen, and A. Jørstad, 2008, Shale rock physics and implications for AVO analysis: A North Sea demonstration: The Leading Edge, **27**, no. 6, 788–797, http://dx.doi.org/10.1190/1.2944164.

Avseth, P., A. Janke, and F. Horn, 2016, AVO inversion in exploration — Key learnings from a Norwegian Sea prospect: The Leading Edge, **35**, no. 5, 405–414, http://dx.doi.org/10.1190/tle35050405.1.

Bredesen, K., E. H. Jensen, T. A. Johansen, and P. Avseth, 2015, Seismic reservoir and source-rock analysis using inverse rock-physics modeling: A Norwegian Sea demonstration: The Leading Edge, **34**, no. 11, 1350–1355, http://dx.doi.org/10.1190/tle34111350.1.

Cooke, D., and J. Cant, 2010, Model-based seismic inversion: Comparing deterministic and probabilistic approaches: CSEG Recorder, **35**, no. 4, 29–39.

Johansen, T. A., E. H. Jensen, G. Mavko, and J. Dvorkin, 2013, Inverse rock physics modeling for reservoir quality prediction: Geophysics, **78**, no. 2, M1–M18, http://dx.doi.org/10.1190/geo2012-0215.1.

Mavko, G., T. Mukerji, and J. Dvorkin, 2009, The rock physics handbook: Tools for seismic analysis of porous media, 2nd ed.: Cambridge University Press, http://dx.doi.org/10.1017/CBO9780511626753.

Smith, G. C., and P. M. Gidlow, 1987, Weighted stacking for rock property estimation and detection of gas: Geophysical Prospecting, **35**, no. 9, 993–1014, http://dx.doi.org/10.1111/j.1365-2478.1987.tb00856.x.

Tarantola, A., 2005, Inverse problem theory and methods for model parameters estimation: SIAM, http://dx.doi.org/10.1137/1.9780898717921.